

## Supplementary Information

### Modified preparation of Si@C@TiO<sub>2</sub> porous microspheres as anodes for high-performance lithium-ion batteries

Jian Luo<sup>a</sup>, Peng Xiao<sup>\*a,b</sup>, Yangjie Li<sup>a</sup>, Jiangzhi Xiong<sup>a</sup>, Peng Zhou<sup>a</sup>, Liang Pang<sup>a</sup>, Xilei Xie<sup>a</sup>, and Yang Li<sup>a,b</sup>

<sup>a</sup> Powder Metallurgy Research Institute, Central South University, Changsha 410083,  
P. R. China.

<sup>b</sup> National Key Laboratory of Science and Technology for National Defence on High-strength Structural Materials, Central South University, Changsha 410083, P. R. China.

\* Corresponding author.

E-mail address: xiaopeng@csu.edu.cn (Peng Xiao)

Tel: +0086-13337311638

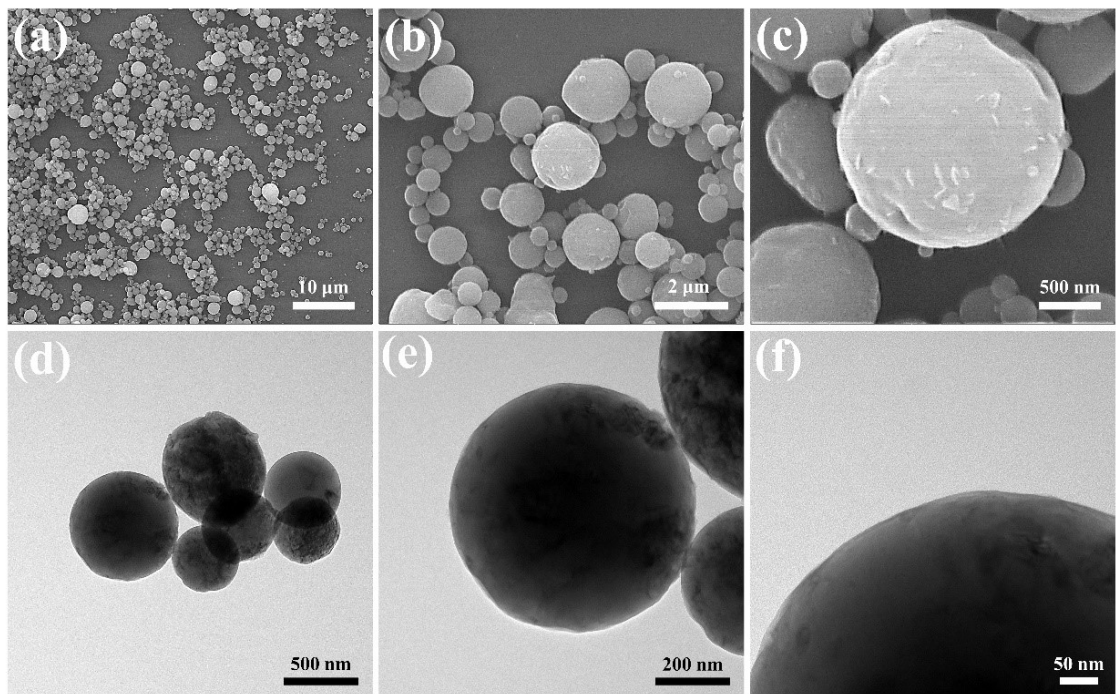


**Figure S1.** SEM and TEM images of the Al-Si powders.

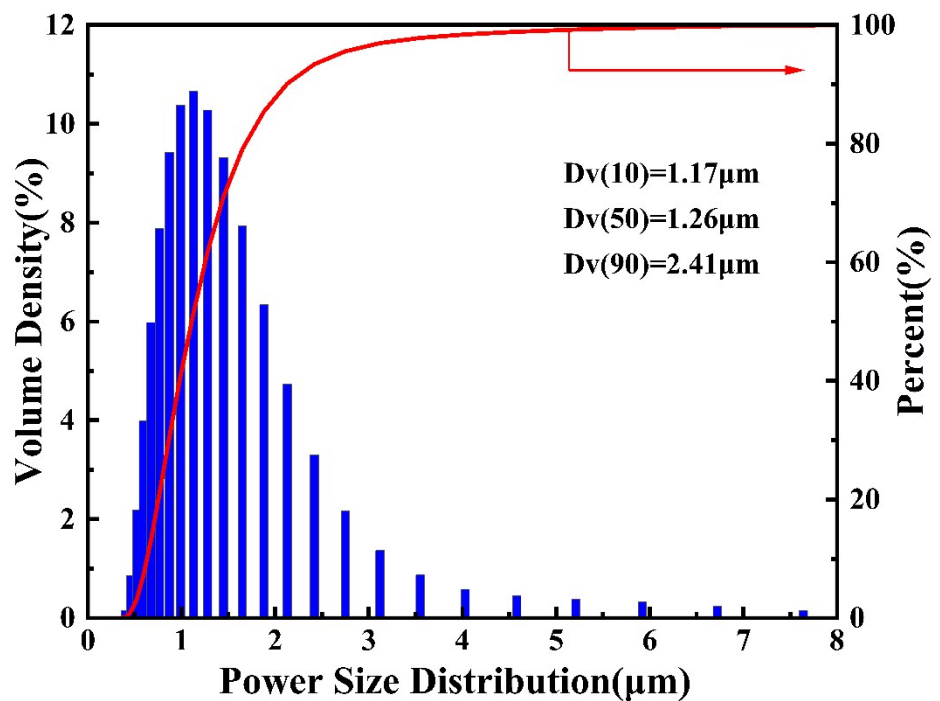


**Figure S2.** Particle size distribution of the Al-Si powders.

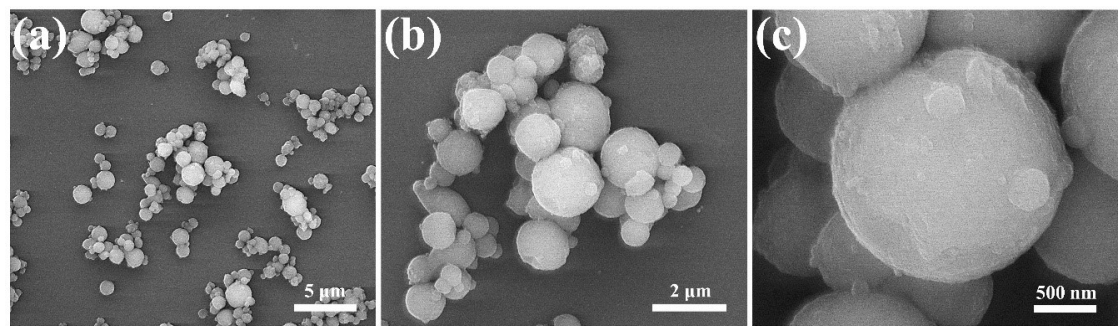


**Figure S3.** SEM images of the Al-Si@RF microspheres.

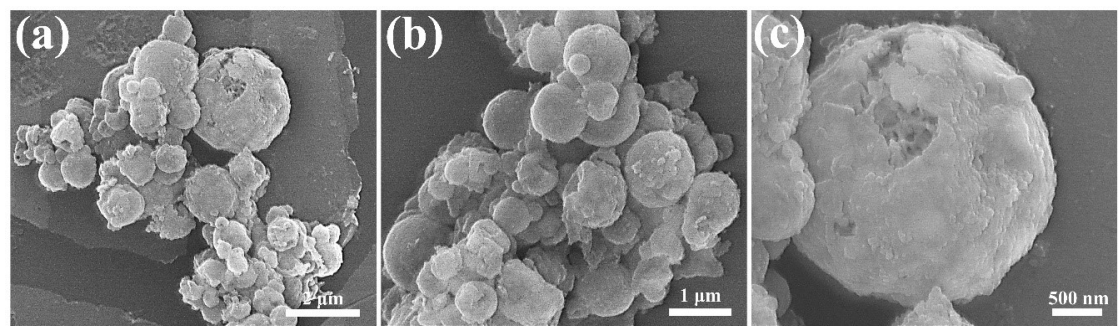


**Figure S4.** SEM images of the PSi@RF microspheres.

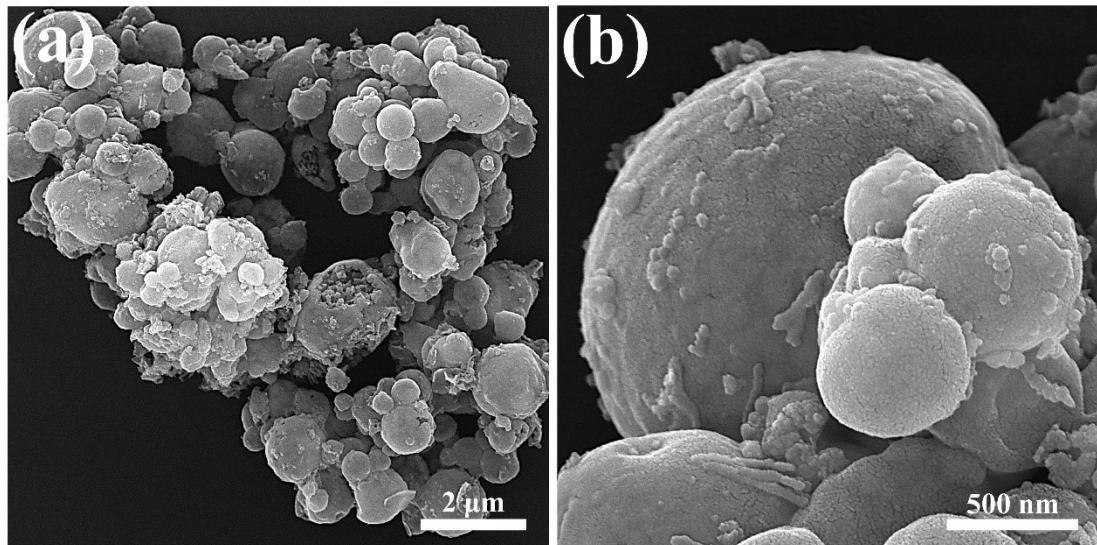


**Figure S5.** SEM images of the PSi@C microspheres.

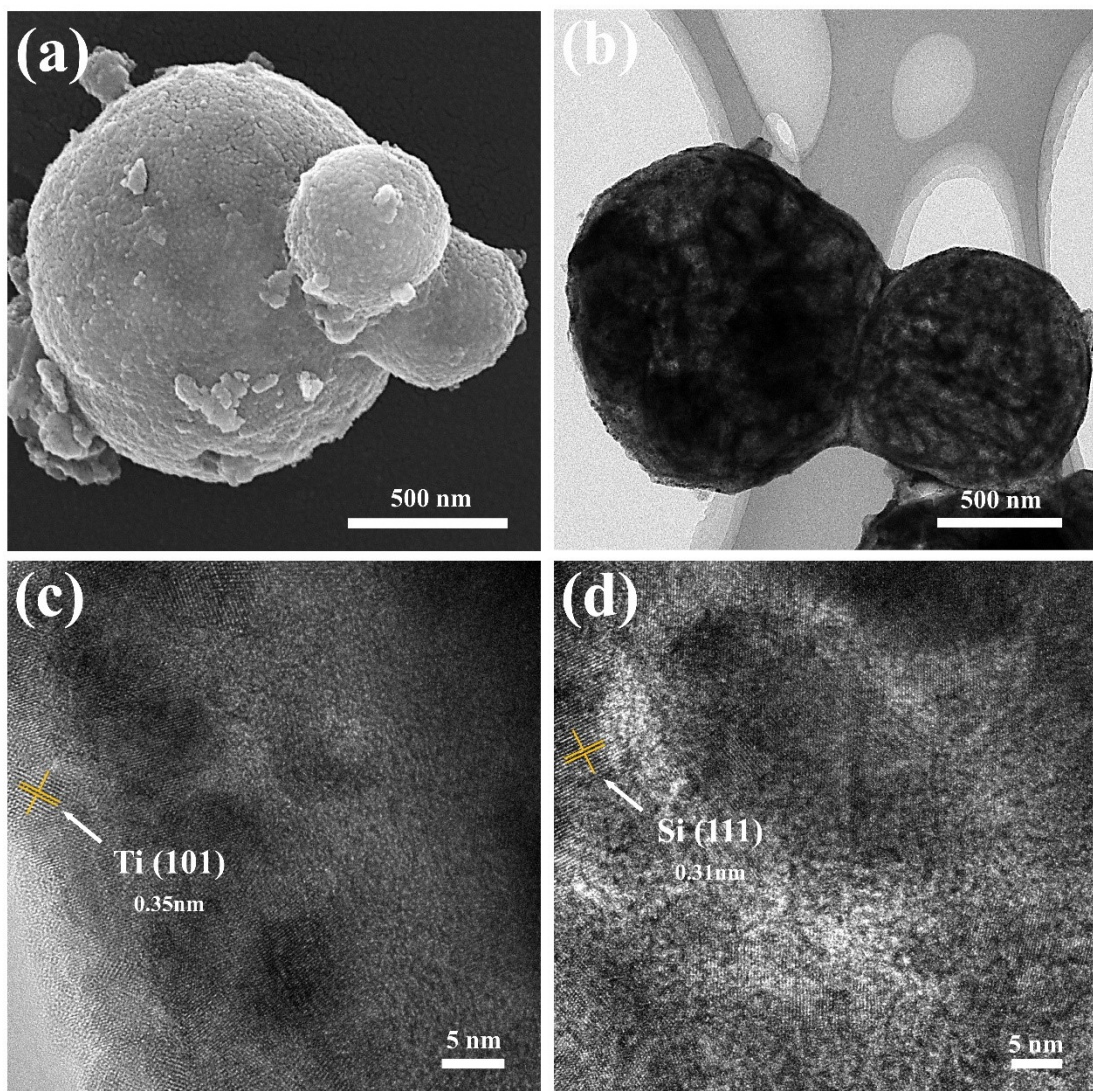


**Figure S6.** SEM and TEM images of the PSi@C@TiO<sub>2</sub> microspheres.

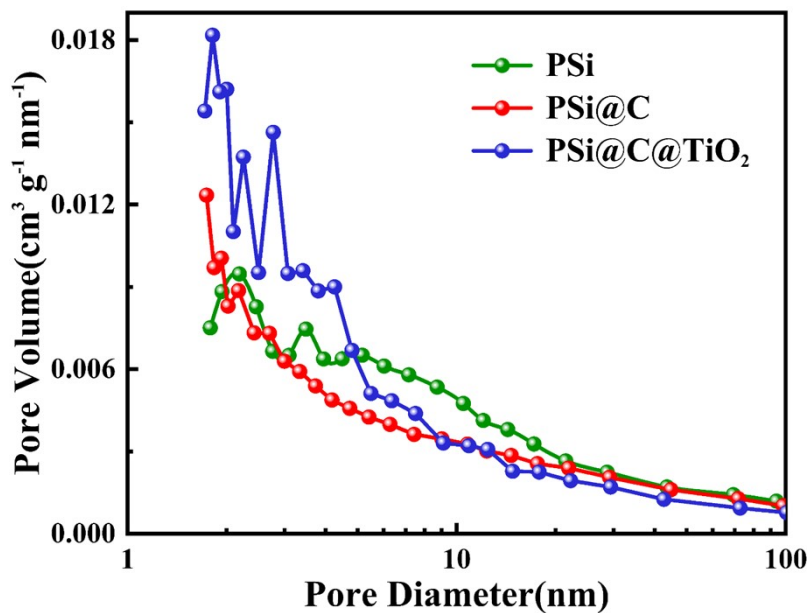


**Figure S7.** The pore size distribution diagrams of the PSi, PSi@C and PSi@C@TiO<sub>2</sub> microspheres.

**Table S1.** Geometric parameters of sample. (Total surface:  $S_{\text{BET}}$ ; Volume of pores in the range of 1.7–300 nm in diameter:  $V_{1.7-300 \text{ nm}}$ ; Average pore size:  $P_{\text{BJH}}$ ).

Samples	$S_{\text{BET}}$ ( $\text{m}^2 \text{ g}^{-1}$ )	$V_{1.7-300 \text{ nm}}$ ( $\text{cm}^3 \text{ g}^{-1}$ )	$P_{\text{BJH}}$ (nm)
PSi	68.7	0.293	10.7
PSi@C	143.2	0.268	16.8
PSi@C@TiO <sub>2</sub>	125.3	0.255	12.5

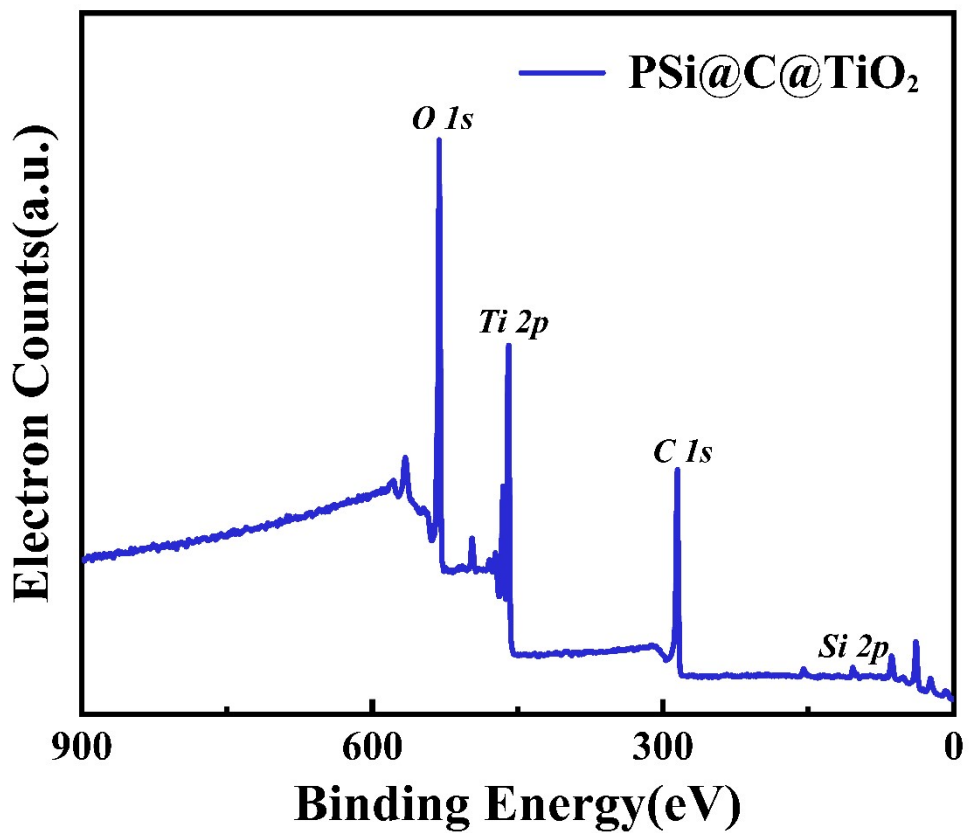


**Figure S8.** XPS survey of the PSi@C@TiO<sub>2</sub> microspheres.

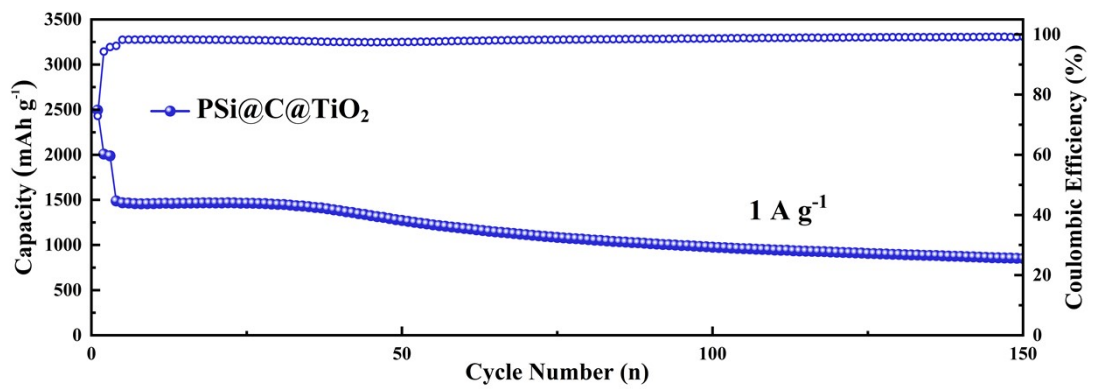


**Figure S9.** The cycling performance of the  $\text{PSi}@\text{C}@\text{TiO}_2$  electrode at  $0.1 \text{ A g}^{-1}$  for the first three cycles and  $1 \text{ A g}^{-1}$  for the subsequent cycles.

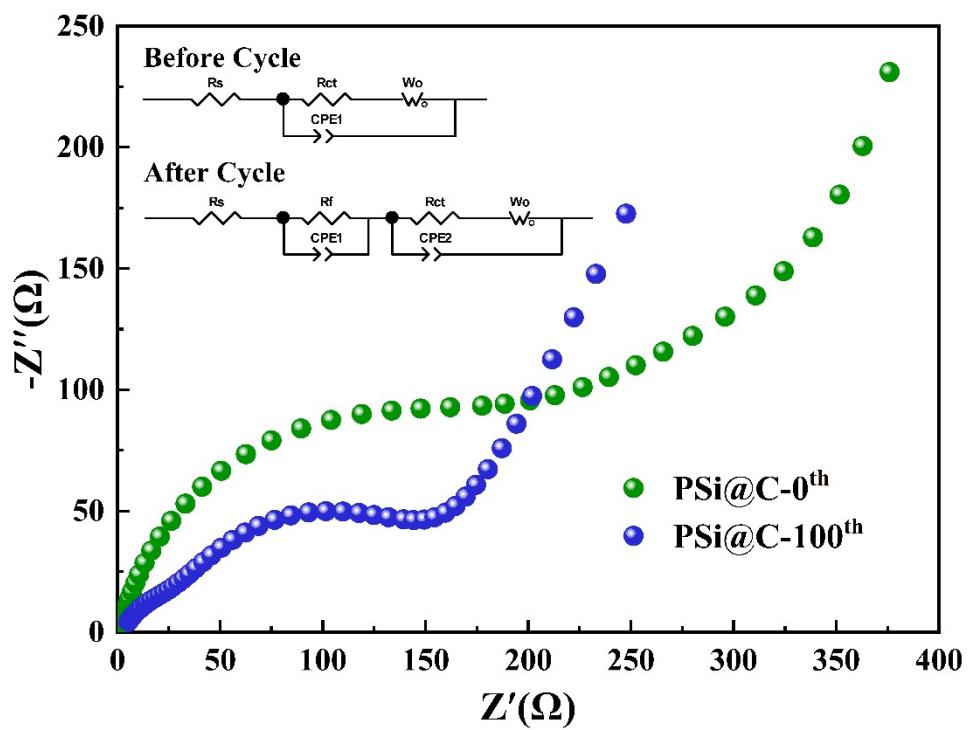


**Figure S10.** Nyquist plots and equivalent circuits of the  $PSi@C$  electrode at different cyclic states.

**Table S2.** Electrode kinetic parameters calculated by fitting the EIS curves in Fig. 5f and Fig. S10.

Cycle number	Resistance	PSi	PSi@C	PSi@C@TiO <sub>2</sub>
<b>Before cycle</b>	$R_s(\Omega)$	1.245	1.328	1.093
	$R_{ct}(\Omega)$	141.5	177	92.08
<b>After 100 cycles</b>	$R_s(\Omega)$	5.284	2.615	2.175
	$R_f(\Omega)$	35.38	26.19	7.909
	$R_{ct}(\Omega)$	159.9	124.4	26.05

**Table S3.** The electrochemical performance of the PSi@C@TiO<sub>2</sub> microspheres and other reported Si-based materials as anodes for LIBs.

Materials	Content of Si (%)	Cycling performance (mAh g <sup>-1</sup> )	Rate capacity (mAh g <sup>-1</sup> )	ICE (%)	Electrode thickness swelling	Refs.
Porous Si sponge	40	570 after 1000 cycles at 1 A g <sup>-1</sup>	410 at 4.2 A g <sup>-1</sup>	56	30%	<sup>1</sup>
TC-SiO	-	674.5 after 100 cycles at 0.14 A g <sup>-1</sup>	~800 at 1.4 A g <sup>-1</sup>	71.9	-	<sup>2</sup>
SiO <sub>x</sub> -TiO <sub>2</sub> @C	70.6 (SiO <sub>x</sub> )	910 after 200 cycles at 0.1 A g <sup>-1</sup>	542 at 3.2 A g <sup>-1</sup>	62.5	-	<sup>3</sup>
Hollow Si@TiO <sub>2</sub> @C	67.2	1270 after 250 cycles at 1 A g <sup>-1</sup>	730 at 8 A g <sup>-1</sup>	86.0 6	45.6%	<sup>4</sup>
Compacted SiO <sub>x</sub> /G/C granules	31	487 after 500 cycles at 0.3 A g <sup>-1</sup>	610 at 3 A g <sup>-1</sup>	84.3	13.7%	<sup>5</sup>
Si@TiO <sub>2</sub>	~95	1580 after 50 cycles at 0.42A g <sup>-1</sup>	-	80.8	-	<sup>6</sup>
Si@TiO <sub>2</sub> /NC	-	1070 after 100 cycles at 0.2 A g <sup>-1</sup>	627 at 3 A g <sup>-1</sup>	75.9	-	<sup>7</sup>
p-SiO <sub>x</sub> @TiO <sub>2</sub> @C	~44	801 after 100 cycles at 0.28 A g <sup>-1</sup>	414 at 7 A g <sup>-1</sup>	67	20%	<sup>8</sup>
Si/C@TiO <sub>2</sub>	53	1077 after 100 cycles at 0.2 A g <sup>-1</sup>	749.4 at 5 A g <sup>-1</sup>	75	-	<sup>9</sup>
PSi@C@ TiO <sub>2</sub>	65.2	1041 after 250 cycles at 0.5 A g <sup>-1</sup>	745 at 5 A g <sup>-1</sup>	73	35.3%	In this work

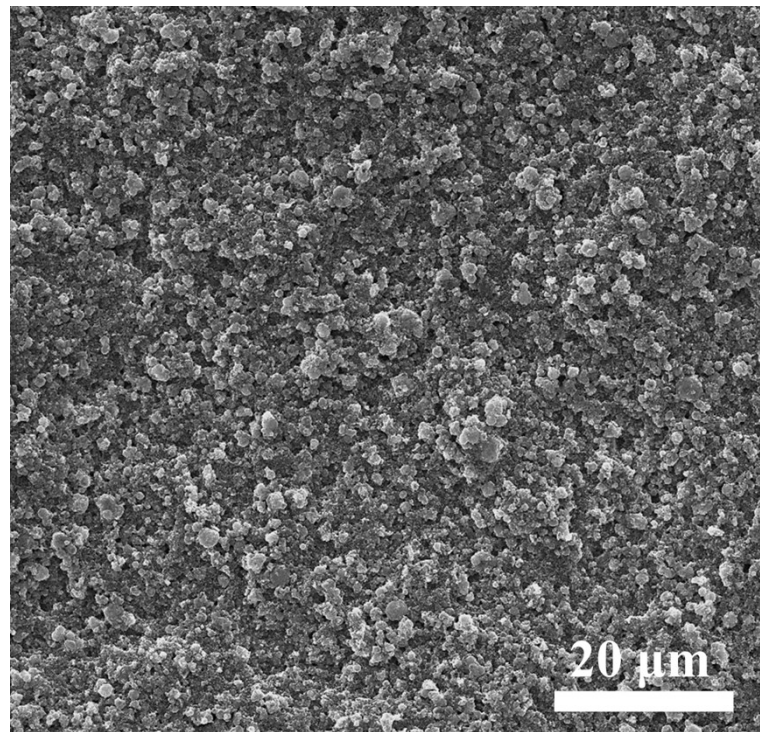


**Figure S11.** SEM images of the pristine PSi@C@TiO<sub>2</sub> electrode.

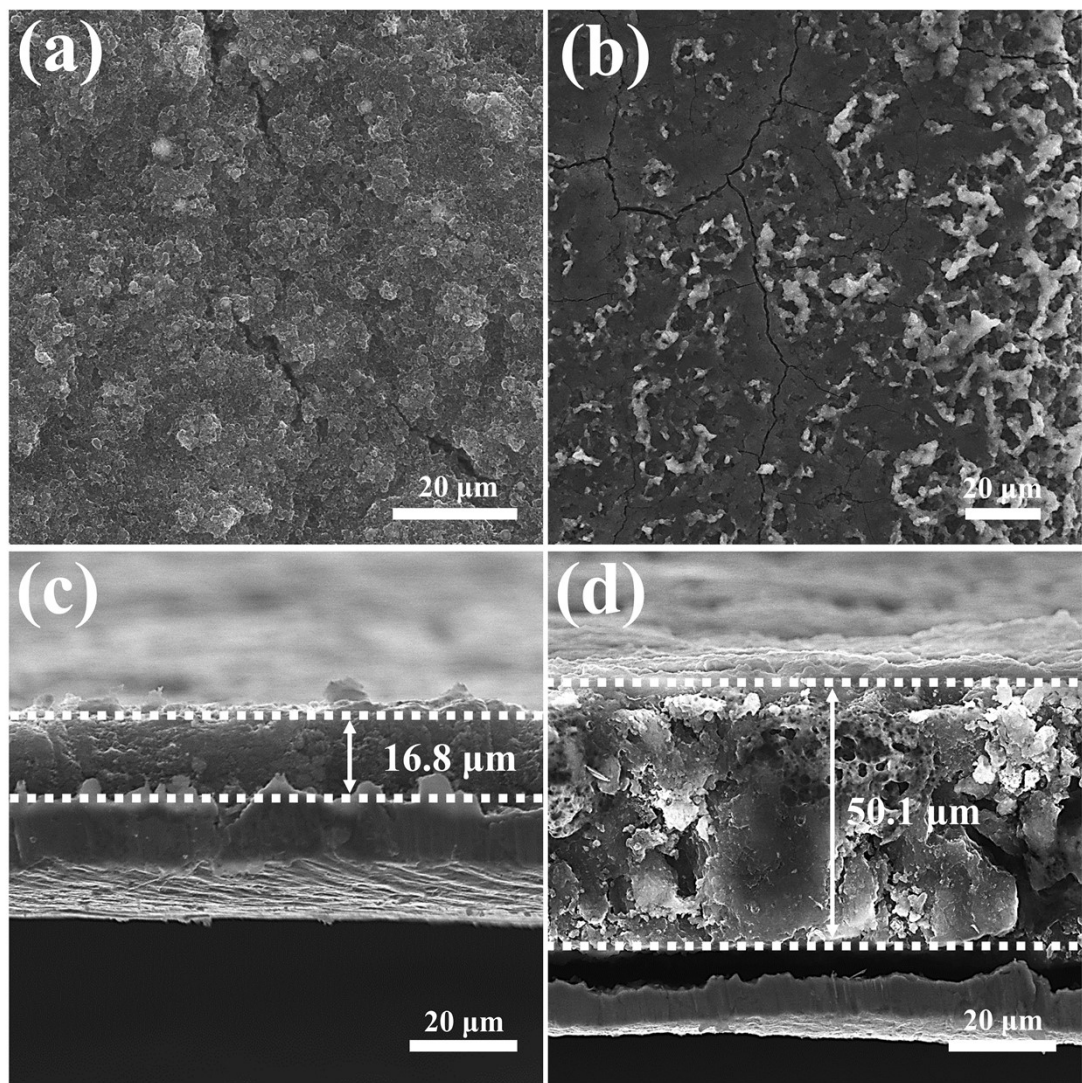


**Figure S12.** SEM images of the PSi@C electrode after 100 cycles (a-b). Cross-sectional SEM image of the PSi@C electrode: before cycling (c) and after 100 cycles (d) at  $0.5 \text{ A g}^{-1}$ .

## **References:**

1. X. Li, M. Gu, S. Hu, R. Kennard, P. Yan, X. Chen, C. Wang, M. J. Sailor, J.-G. Zhang and J. Liu, *Nat. Commun.*, 2014, **5**, 4105.
2. F. Dou, L. Shi, P. Song, G. Chen, J. An, H. Liu and D. Zhang, *Chem. Eng. J.*, 2018, **338**, 488-495.
3. Z. Li, H. Zhao, P. Lv, Z. Zhang, Y. Zhang, Z. Du, Y. Teng, L. Zhao and Z. Zhu, *Adv. Funct. Mater.*, 2018, **28**.
4. B. Lu, B. Ma, X. Deng, B. Wu, Z. Wu, J. Luo, X. Wang and G. Chen, *Chem. Eng. J.*, 2018, **351**, 269-279.
5. G. Li, J.-Y. Li, F.-S. Yue, Q. Xu, T.-T. Zuo, Y.-X. Yin and Y.-G. Guo, *Nano Energy*, 2019, **60**, 485-492.
6. Y. Bai, D. Yan, C. Yu, L. Cao, C. Wang, J. Zhang, H. Zhu, Y.-S. Hu, S. Dai, J. Lu and W. Zhang, *J. Power Sources*, 2016, **308**, 75-82.
7. R. Fang, W. Xiao, C. Miao, P. Mei, Y. Zhang, X. Yan and Y. Jiang, *Electrochim. Acta*, 2019, **317**, 575-582.
8. F. Dou, Y. Weng, G. Chen, L. Shi, H. Liu and D. Zhang, *Chem. Eng. J.*, 2020, **387**.
9. Z. Yi, N. Lin, T. Xu and Y. Qian, *Chem. Eng. J.*, 2018, **347**, 214-222.